Optically Guided Beam Splitter for Propagating Matter Waves

G. L. Gattobigio,[1,2] A. Couvert,[2] G. Reinaudi,[2,3] B. Georgeot,[4,5] and D. Guéry-Odelin[1,2]

[1]*Laboratoire de Collisions Agrégats Réactivité, CNRS UMR 5589, IRSAMC, Université Paul Sabatier, 118 Route de Narbonne, 31062 Toulouse CEDEX 4, France*

[2]*Laboratoire Kastler Brossel, Ecole Normale Supérieure, 24 rue Lhomond, 75005 Paris, France*

[3]*Department of Physics, Columbia University, 538 West 120th Street, New York, New York 10027, USA*

[4]*Laboratoire de Physique Théorique (IRSAMC), Université de Toulouse (UPS), 31062 Toulouse, France*

[5]*CNRS, LPT UMR5152 (IRSAMC), 31062 Toulouse, France*

(Received 5 March 2012; revised manuscript received 21 May 2012; published 19 July 2012)

We study experimentally and theoretically a beam splitter setup for guided atomic matter waves. The matter wave is a guided atom laser that can be tuned from quasimonomode to a regime where many transverse modes are populated, and propagates in a horizontal dipole beam until it crosses another horizontal beam at 45°. We show that depending on the parameters of this X configuration, the atoms can all end up in one of the two beams (the system behaves as a perfect guide switch), or be split between the four available channels (the system behaves as a beam splitter). The splitting regime results from a chaotic scattering dynamics. The existence of these different regimes turns out to be robust against small variations of the parameters of the system. From numerical studies, we also propose a scheme that provides a robust and controlled beam splitter in two channels only.

DOI: 10.1103/PhysRevLett.109.030403 PACS numbers: 03.75.Kk, 05.45.−a, 37.10.Gh, 67.85.−d

Matter-wave interferometry has the potential of being several orders of magnitude more sensitive than optical interferometry. Many demonstrations have been made of its use for high-precision gravimeters or gyrometers [1]. Its development requires the coherent manipulation of matter waves with atom optical elements. In this respect, the achievement of beam splitters for atoms moving in free space was essential [2–8].

To optimize the sensitivity of an atomic interferometer, one needs large angle beam splitters with atom wave packets having a narrow momentum distribution [9]. A few strategies are currently being explored or envisioned to increase the enclosed area: the enhancement of the interaction time based on a large momentum beam splitter [7,8,10], atom interferometry experiments placed in a reduced gravity environment [11,12], or the use of slow atoms in a guided environment.

In this Letter, we shed light on the physics of matter-wave splitting in a crossing guide configuration. Confined geometries for atom interferometry are promising in terms of compactness and portability. A wide variety of techniques is available for designing potentials and guides for the external degrees of freedom, and they have been used to investigate the operation mode of different types of beam splitters. One should distinguish between those involving a trap [10,13–18] and those based on combinations of waveguides [19–23]. So far, the former have been investigated in the Bose-Einstein condensate (BEC) regime, while the latter were studied in the thermal regime. In this Letter we report on the experimental and theoretical study of an all-optical beam splitter structure for propagating matter waves in both regimes (i.e., initial populations in the transverse modes vary from the thermal multimode to the monomode limit [24]). This problem amounts to a quantum scattering problem in a confined environment in which chaotic behavior can emerge [25–27].

The beam splitter is obtained by combining two guides which provide a potential structure where four paths are available for the matter wave. In our experimental setup, we use two dipole beams crossing at 45° in a horizontal plane (see Fig. 1). This X configuration has four channels [28,29]. Optical confinement has many advantages: it can be applied to atoms with no permanent magnetic moment (e.g., ytterbium and alkaline-earth), which is particularly interesting for metrology, an extra magnetic field can be used to tune the interactions (Feshbach resonance) or apply an external force, and the focus position can be easily moved [30,31]. Furthermore, the crossing region has a confinement strength larger than that of the guides. As a

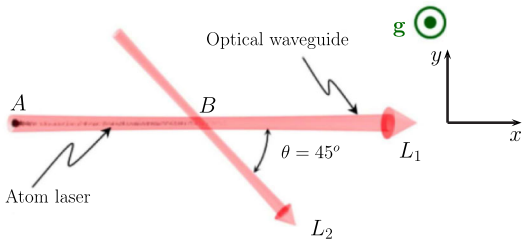

FIG. 1 (color online). Schematic of the matter-wave guided beam splitter setup based on two crossing dipole beams in a horizontal plane (**g** denotes the gravity vector). Atoms are outcoupled from a BEC located at point A and propagate in the guide provided by beam L_1 towards point B where beam L_2 crosses beam L_1.

result the setup is robust against low frequency noise. This is to be contrasted with Y geometries where the connection zone between the guides implies an important lowering of the potential strength [19–21,32].

We produce a rubidium-87 BEC in a crossed dipole trap using two focused red-detuned laser beams (wavelength of 1070 nm, i.e., detuning of 100 THz, waist of $w_1 \simeq 35$ μm) [24]. The second crossed dipole beam forming the BEC trap at point A is not shown in Fig. 1 since it is out of the plane. Beams L_1 and L_2 originate from the same laser but have a frequency difference of 80 MHz to wash out possible interferences. Atoms are prepared in the $|F = 1, m_F = 0\rangle$ internal state through a spin distillation process implemented during the evaporative cooling stage [33]. The guided atom lasers are realized by outcoupling atoms from the BEC in the horizontal dipole beam of the trap, either by applying a time-dependent magnetic field gradient or by reducing the intensity of the nonhorizontal beam of the crossing dipole trap [24,33–37].

Although atom-atom interactions may not always dramatically alter the coherence [38], theoretical studies of cold atoms interferometers based on guiding potentials show that they can dramatically affect the contrast of the expected interference signal [39,40]. To reduce the role played by interactions we perform the outcoupling very slowly. The low atomic density of the propagating beam makes this system nearly interaction-free [24,33]. The propagating matter wave is characterized by its atom flux ($\sim$ few10^5 atoms/s), its mean velocity (13 ± 2 mm $\cdot$ s^{-1}) and the mean excitation number $\langle n \rangle$ associated with the transverse modes. $\langle n \rangle$ can be tuned at will using the protocol detailed in [24]: First, the fraction of condensed atoms is adjusted by controlling the final stage of the evaporation ramp, and second a quasi-isentropic outcoupling of the atoms from the trap to the guide is performed by decreasing the trap depth very slowly with respect to the trap and guide frequencies [41]. For $\langle n \rangle = 10$ more than hundreds of transverse levels are populated (since one has to take into account the degeneracy), while one transverse state is populated for $\langle n \rangle = 0$.

After evaporation the power of beam L_1 is raised up to $P_1 = 140$ mW and kept constant thereafter. This corresponds to a measured transverse frequency of the guide of about 300 Hz and a depth of 10 μK. The crossing beam L_2 has a waist $w_2 = 70 \pm 5$ μm and an adjustable power P_2. Atoms propagate for a time long enough to obtain clear information on the asymptotic output channels. In practice, the crossing between L_1 and L_2 beams is at 700 μm downstream from the BEC trap. The beam propagates during 200 ms, and we take an absorption picture after a time of flight of a few ms.

In a first set of experiments, we prepare the propagating guided atom laser in the ground state of the transverse confinement ($\langle n \rangle \simeq 0$). We observe three different regimes, (I), (II), and (III), depending on P_2/P_1 (see Fig. 2). Images (I) belong to the weak defect regime for which the beam is transversely excited after passing through the

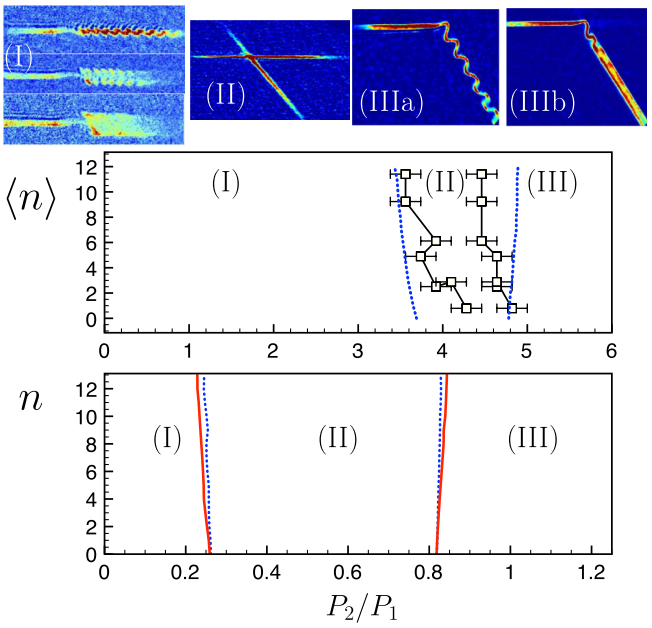

FIG. 2 (color online). Propagation of an atom laser in an X shape guide structure. Top: Three regimes are experimentally observed depending on the power ratio, P_2/P_1, of the guides: (I) weak defect regime where the excitation of transverse modes downstream from the crossing increases with P_2/P_1, (II) splitting regime where atoms explored all the available channels, and (IIIa, IIIb) switch regime where all atoms are directed into guide L_2. The mean initial transverse excitation numbers of the incoming beam are $\langle n \rangle \simeq 0.3$ (IIIa) and $\langle n \rangle \simeq 10$ (IIIb). Middle: Experimental diagram that summarizes the observed regime depending on both the power ratio P_2/P_1 and the mean initial transverse populations. The boundaries of the three regimes turn out to be robust against the population of the transverse modes. The blue dotted line shows full three-dimensional classical simulations for $w_1 = 40$ μm, $w_2 = 72$ μm, wave packets started 700 μm before the crossing, with an acceleration of 0.2 m $\cdot$ s^{-2}, and a vertical misalignment of crossing beams of 2 μm. Bottom: Numerical simulations with other parameters confirming the existence of the three regimes and the robustness of the boundaries against n; red solid line: quantum simulations, blue dotted line: classical simulations. Wave packets are started 150 μm before the crossing, with initial longitudinal velocity 10 mm.s^{-1}, for $w_1 = 45$ μm, $w_2 = 41$ μm.

interaction region. The coherent excitation of the transverse modes is induced by the weak coupling between the longitudinal and transverse degrees of freedom in the crossing guide region. As illustrated in images (I) of Fig. 2, the larger P_2/P_1, the stronger the coupling and the larger the number of transverse modes populated downstream. Image (II) corresponds to the splitting regime where atoms can explore the four channels provided by our X shape geometry. It corresponds to a much stronger coupling between the different degrees of freedom and the corresponding classical dynamics becomes chaotic (see below) [27,42,43]. Images (III) illustrate the switch regime where atoms go into one arm of the beam L_2 with a 100% efficiency [20,21]. The center of mass motion is excited as

a result of momentum transfer of the longitudinal incident momentum to the transverse degrees of freedom of the output channel guide.

We also have experimentally investigated this dynamics for various values of the initial mean quantum number $\langle n \rangle$ of the transverse states [24]. In Fig. 2 (middle) we plot the line representing the boundary between (I) and (II) where (I) is defined by more than 80% of the atoms continuing to propagate in the original guide L_1. Also plotted is the boundary between (II) and (III) where (III) is defined by more than 80% of the atoms being deviated to the guide L_2. The error bars show the typical size of the transition regions.

The three regimes are still present even if many transverse states are populated. However, the transverse oscillations can be observed only for low incoming mean transverse excitation [compare images (IIIa) and (IIIb) taken for different values of $\langle n \rangle$]. In previous experiments where the splitting of a beam of cold atoms was carried out, it was impossible to observe this transverse excitation since many transverse states were populated and these oscillations were thus washed out [19,20,22,23]. The boundaries between the different regimes appear to be very robust against $\langle n \rangle$ and a slight misalignment of the crossing beam. This is to be contrasted with the interaction of a guided atom laser with an out-of-center vertical potential [27]. The boundaries remain nearly unchanged when the crossing is misaligned by a tenth of the waist of the beams. For each set of data the alignment was checked before and after the data acquisition. We estimate that the maximum relative change of the beam vertical positions is below 2 μm.

To interpret the splitting regime, we have computed the dynamics of 2D quantum wave packets using the split-Fourier algorithm [44] and developed a direct simulation Monte Carlo method where atoms are evolved according to classical mechanics [see Fig. 2 (bottom)]. The three regimes observed experimentally can be reproduced by numerical simulations and turn out to be generic. Each point in Fig. 2 (bottom) corresponds to the results obtained for an initial state that coincides with the nth transverse eigenstate. We observe that the boundaries deduced from classical and quantum simulations are very close. The fact that the boundaries are not exactly the same in classical and quantum dynamics is somewhat expected since the equations fulfilled by the center of mass of the wave packet are different in classical and quantum mechanics. Indeed, the external potential is no longer harmonic in the crossing guide region. The error bars on the experimental data are such that one cannot distinguish the classical from the quantum nature of the motion at low n. Numerical studies confirm that despite the presence of chaotic dynamics, the existence of the boundaries between the different regimes is robust. However, their precise positions can depend on several parameters such as small misalignment of the crossing beams, a residual longitudinal acceleration and/or the beams characteristics (M^2 factor, waist, residual astigmatism, etc.). Many of these parameters cannot be measured accurately. As an example, we show in Fig. 2 (middle) the result of full classical three-dimensional simulations with a certain set of parameters which agree well with the experimental data.

Figure 3 provides a typical experimental example of the dynamics of the splitting regime. The guided atom laser that enters the crossing region remains partially trapped (larger density) and then the contamination of all available branches is observed, until all the atoms have left the scattering region. We have plotted in Fig. 4 the output channels obtained from a simulation relying on classical mechanics (using different colors for the different output channels) for different initial conditions of the transverse phase space. We clearly identify a chaotic region with a fractal structure in which a very small change in the initial condition changes the output channel [25]. We have also checked that Lyapunov exponents become positive in this parameter region. To further characterize this zone, we have verified that the set of boundaries between the four accessible output channels as a function of the initial conditions displays a fractal structure. For a wide variety of fixed transverse velocity v_y in regime (II), we find a fractal dimension of $\xi \simeq 0.85$, revealing a strong fractality of the basin boundaries, usually associated with chaotic scattering. Furthermore, our numerical studies seem to indicate that the fractal Wada property [25,45,46] can be fulfilled in this system. The distribution of trapping times in the vicinity of the crossing guide region is found to exhibit an exponential decay.

Interestingly the population in a given channel can be reduced by adding a small extra gradient; this happens in the experiment if the beams are not perfectly horizontal. In our nearly horizontal configuration, a gradient that corresponds to a hundredth of gravity strength is sufficient to dramatically dissymmetrize the population in the output channels. In this way one can populate only two channels and realize a two-channel beam splitter. This effect has been checked numerically and explains the variation of the populations in the different channels seen in the experimental results [compare image (II) of Fig. 2 and images of

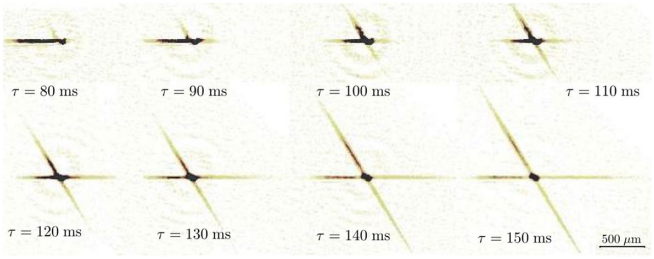

FIG. 3 (color online). Example of experimental splitting dynamics illustrating regime (II) (see Fig. 2). Time evolution is directly visible in the succession of absorption images (taken after a 400 μs time of flight). The mean velocity is 10 mm/s. The images show a larger density at the crossing point which is attributed to the complex dynamics that traps the atoms there for some time. Atoms that escape from this region populate all available channels.

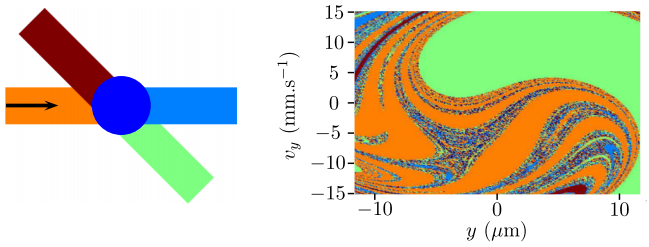

FIG. 4 (color online). Left: Colors associated with the different output channels. The arrow indicates the propagation direction of the incoming atoms. The overlap region between the guide is represented as a dark blue disk. Right: Output channels associated to different initial phase space conditions of the transverse degree of freedom in regime (II) (see Fig. 2). Each classical trajectory started at the bottom of the guide, 150 μm before the crossing, with initial velocity 10 mm $\cdot$ s^{-1}, for $w_1 = 45$ μm, $w_2 = 41$ μm, $P_2 = 0.143$ $W = 0.8P_1$.

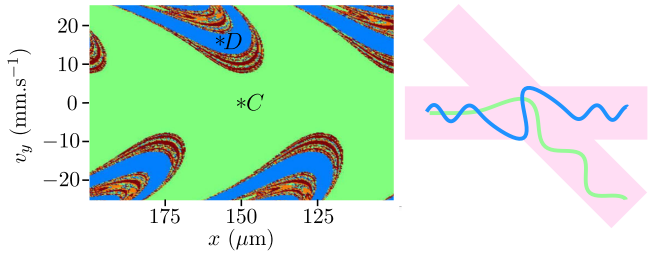

FIG. 5 (color online). Left: Output channels for a classical trajectory started at the bottom of the guide, between 100 μm and 200 μm before the crossing, with initial longitudinal velocity 10 mm $\cdot$ s^{-1}, and an initial transverse velocity between -25 mm $\cdot$ s^{-1} and 25 mm $\cdot$ s^{-1}, with $w_1 = 45$ μm, $w_2 = 41$ μm, $P_2 = 0.365$ $W = 2.04P_1$. Right: Center of mass motion of numerically simulated quantum wave packets. The one with the initial parameters of point C (150 μm before defect, no transverse velocity) is deviated in the second guide at 99.9% (green curve). In contrast, the one with the initial parameters of point D (154.75 μm before defect, transverse velocity of 15.5 mm $\cdot$ s^{-1}) ends up at 96.2% in the initial beam (blue curve).

Fig. 3]. A beam splitter experiment for a thermal cloud accelerated by gravity in a quasivertical configuration has been discussed in [22,47]. The possibility of realizing a coherent beam splitter using the transient dynamics of a chaotic system has been addressed in another context with amplitude modulated optical lattices [48].

In view of applications in atomic interferometry in guided geometries, we further discuss a few features of our setup. First, the split beams in each output guide undergo a transverse oscillation [see images (III) of Fig. 2]. Numerical studies indicate that an out-of-guide axis potential with an appropriate strength can be used to remove this remaining transverse dipole oscillation [27]. Second, one may wonder about the control of the relative phase of the beams in the different output channels for a chaotic beam splitter. Although a high precision control of experimental conditions is certainly mandatory, it should be achievable with state of the art techniques since the chaotic potential affects the atoms only for a short time. In the context of a Mach-Zehnder interferometer, a symmetric scheme could circumvent this problem using for instance the same beam splitter at the entrance and the exit provided an appropriate mirror in guided geometries can be achieved. Alternatively, one can implement a beam splitter that does not rely on chaos.

In the following, we propose such a scheme using a transverse momentum kick transferred to atoms before they enter the crossing region. The power ratio is chosen to be in regime (III) (the switch guide regime). Different experimental techniques can be used to achieve such a transfer: Bragg or Raman transitions, Bloch oscillations [49]. In our simulation, we add an instantaneous transverse momentum upstream to account for the momentum kick. Figure 5 summarizes our numerical results. Each asymptotic output channel obtained here from a classical simulation is represented by a different color as a function of the velocity kick value and the "phase", i.e., the position before the crossing at which the momentum transfer is performed. Using the prediction of the simulations relying on classical physics as guidelines for quantum simulations, we confirm the feasibility of redirecting atoms in guide L_1 with an efficiency larger than 96%. This technique enables one to switch from guide L_2 to L_1 without changing the guide characteristics in time [20,21]. This also means that if the incoming wave packet is prepared in a linear superposition with equal weight of the states with and without the proper transverse momentum kick, the wave function can be split into two coherent wave packets that propagate in the two guides L_1 and L_2. Interestingly enough, the domain of useful parameters in the momentum kick and phase to realize such a guided matter-wave beam splitter is relatively large.

In conclusion, this Letter reports on the realization of all-optical guided beam splitter devices. Such tools are important for the development of guided atomic optics with a huge potential for applications, in particular for inertial sensors. In addition, there exists a direct mapping between waveguide theory and space-time trajectories of spin chain transport in which the virtual guide to conduct spin excitations is produced by a spatially and time varying potential applied onto a 1D spin chain [50]. This opens possible applications of our scheme in solid state quantum information transport.

We thank J. Vigué for useful discussions, R. Mathevet and T. Lahaye for useful comments at the early stage of this work, and J. Palmeri for a careful reading of the manuscript. We acknowledge financial support from the Agence Nationale de la Recherche (GALOP project), the Région Midi-Pyrénées, the university Paul Sabatier (OMASYC project), the NEXT project ENCOQUAM and the Institut Universitaire de France. We thank CalMiP for the use of their supercomputers.

[1] A. D. Cronin, J. Schmiedmayer and D. E. Pritchard, Rev. Mod. Phys. **81**, 1051 (2009).

[2] Ch. J. Bordé, Ch. Salomon, S. Avrillier, A. van Lerberghe, Ch. Bréant, D. Bassi, and G. Scoles, Phys. Rev. A **30**, 1836 (1984).

[3] P. J. Martin, B. G. Oldaker, A. H. Miklich, and D. E. Pritchard, Phys. Rev. Lett. **60**, 515 (1988).

[4] M. Kasevich and S. Chu, Phys. Rev. Lett. **67**, 181 (1991).

[5] C. Antoine, Appl. Phys. B **84**, 585 (2006).

[6] J. Dugué, G. Dennis, M. Jeppesen, M. T. Johnsson, C. Figl, N. P. Robins, and J. D. Close, Phys. Rev. A **77**, 031603 (2008).

[7] P. Cladé, S. Guellati-Khélifa, F. Nez, and F. Biraben, Phys. Rev. Lett. **102**, 240402 (2009).

[8] H. Müller, S.-w. Chiow, S. Herrmann, and S. Chu, Phys. Rev. Lett. **102**, 240403 (2009).

[9] S. Wu, Y.-J. Wang, Q. Diot, and M. Prentiss, Phys. Rev. A **71**, 043602 (2005).

[10] S.-w. Chiow, T. Kovachy, H.-C. Chien, and M. A. Kasevich, Phys. Rev. Lett. **107**, 130403 (2011).

[11] P. Laurent, P. Lemonde, E. Simon, G. Santarelli, A. Clairon, N. Dimarcq, P. Petit, C. Audoin and C. Salomon, Eur. Phys. J. D **3**, 201 (1998).

[12] C. Salomon *et al.*, C.R. Seances Acad. Sci. Ser. 4 **2**, 1313 (2001).

[13] Y.-J. Wang, D. Z. Anderson, V. M. Bright, E. A. Cornell, Q. Diot, T. Kishimoto, M. Prentiss, R. A. Saravanan, S. R. Segal, and S. Wu, Phys. Rev. Lett. **94**, 090405 (2005).

[14] T. Schumm, S. Hofferberth, L. M. Andersson, S. Wildermuth, S. Groth, I. Bar-Joseph, J. Schmiedmayer, and P. Krüger, Nature Phys. **1**, 57 (2005).

[15] P. Hommelhoff, W. Hänsel, T. Steinmetz, T. W. Hänsch, and J. Reichel, New J. Phys. **7**, 3 (2005).

[16] O. Garcia, B. Deissler, K. J. Hughes, J. M. Reeves, and C. A. Sackett, Phys. Rev. A **74**, 031601(R) (2006).

[17] G.-B. Jo, Y. Shin, S. Will, T. A. Pasquini, M. Saba, W. Ketterle, D. E. Pritchard, M. Vengalattore, and M. Prentiss, Phys. Rev. Lett. **98**, 030407 (2007).

[18] K. Maussang, G. E. Marti, T. Schneider, P. Treutlein, Y. Li, A. Sinatra, R. Long, J. Estève, and J. Reichel, Phys. Rev. Lett. **105**, 080403 (2010).

[19] D. Cassettari, B. Hessmo, R. Folman, T. Maier, and J. Schmiedmayer, Phys. Rev. Lett. **85**, 5483 (2000).

[20] M. J. Renn, D. Montgomery, O. Vdovin, D. Z. Anderson, C. E. Wieman, and E. A. Cornell,Phys. Rev. Lett. **75**, 3253 (1995).

[21] D. Müller, E. A. Cornell, M. Prevedelli, P. D. D. Schwindt, Y.-J. Wang, and D. Z. Anderson, Phys. Rev. A **63**, 041602 (R) (2001).

[22] O. Houde, D. Kadio, and L. Pruvost, Phys. Rev. Lett. **85**, 5543 (2000).

[23] R. Dumke, T. Müther, M. Volk, W. Ertmer, and G. Birkl, Phys. Rev. Lett. **89**, 220402 (2002).

[24] G. L. Gattobigio, A. Couvert, M. Jeppesen, R. Mathevet, and D. Guéry-Odelin, Phys. Rev. A **80**, 041605(R) (2009).

[25] J. Aguirre, R. L. Viana, and M. A. F. Sanjuán, Rev. Mod. Phys. **81**, 333 (2009).

[26] G. L. Gattobigio, A. Couvert, B. Georgeot, and D. Guéry-Odelin, New J. Phys. **12**, 085013 (2010).

[27] G. L. Gattobigio, A. Couvert, B. Georgeot, and D. Guéry-Odelin, Phys. Rev. Lett. **107**, 254104 (2011).

[28] D. C. E. Bortolotti and J. L. Bohn, Phys. Rev. A **69**, 033607 (2004).

[29] H. Kreutzmann, U. V. Poulsen, M. Lewenstein, R. Dumke, W. Ertmer, G. Birkl, and A. Sanpera, Phys. Rev. Lett. **92**, 163201 (2004).

[30] T. L. Gustavson, A. P. Chikkatur, A. E. Leanhardt, A. Görlitz, S. Gupta, D. E. Pritchard, and W. Ketterle, Phys. Rev. Lett. **88**, 020401 (2001).

[31] A. Couvert, T. Kawalec, G. Reinaudi, and D. Guéry-Odelin, Europhys. Lett. **83**, 13 001 (2008).

[32] M. Jääskeläinen and S. Stenholm, Phys. Rev. A **66**, 023608 (2002); **68**, 033607 (2003).

[33] A. Couvert, M. Jeppesen, T. Kawalec, G. Reinaudi, R. Mathevet, and D. Guéry-Odelin, Europhys. Lett. **83**, 50 001 (2008).

[34] W. Guerin, J.-F. Riou, J. P. Gaebler, V. Josse, P. Bouyer, and A. Aspect, Phys. Rev. Lett. **97**, 200402 (2006).

[35] G. Kleine Büning, J. Will, W. Ertmer, C. Klempt, and J. Arlt, Appl. Phys. B **100**, 117 (2010).

[36] R. G. Dall, S. S. Hodgman, M. T. Johnsson, K. G. H. Baldwin, and A. G. Truscott, Phys. Rev. A **81**, 011602(R) (2010).

[37] R. G. Dall, S. S. Hodgman, A. G. Manning, and A. G. Truscott, Opt. Lett. **36**, 1131 (2011).

[38] C. Deutsch, F. Ramirez-Martinez, C. Lacroûte, F. Reinhard, T. Schneider, J. N. Fuchs, F. Piéchon, F. Laloë, J. Reichel, and P. Rosenbusch, Phys. Rev. Lett. **105**, 020401 (2010).

[39] J. A. Stickney and A. A. Zozulya, Phys. Rev. A **66**, 053601 (2002).

[40] S. Chen and R. Egger, Phys. Rev. A **68**, 063605 (2003).

[41] F. Vermersch, C. M. Fabre, P. Cheiney, G. L. Gattobigio, R. Mathevet, and D. Guéry-Odelin, Phys. Rev. A **84**, 043618 (2011).

[42] E. Torrontegui, J. Echanobe, A. Ruschhaupt, D. Guéry-Odelin, and J. G. Muga, Phys. Rev. A **82**, 043420 (2010).

[43] The X configuration that we have investigated thus exhibits two regular regions separated by a chaotic region. Actually, the numerical simulations reveal the existence of other splitting regions at an even higher power ratio P_2/P_1 that were not investigated in our experiment.

[44] The large anisotropy of the wave function (longitudinal size of a few mm and transverse size of a few hundreds of nm) and the long interaction time makes this kind of calculation unrealistic in 3D with the supercomputers currently available.

[45] J. Kennedy and J. A. Yorke, Physica (Amsterdam) **51D**, 213 (1991).

[46] D. Sweet, E. Ott, and J. A. Yorke, Nature (London) **399**, 315 (1999).

[47] N. Gaaloul, A. Suzor-Weiner, L. Pruvost, M. Telmini, and E. Charron, Phys. Rev. A **74**, 023620 (2006).

[48] A. G. Truscott, M. E. J. Friese, W. K. Hensinger, H. M. Wiseman, H. Rubinsztein-Dunlop, and N. R. Heckenberg, Phys. Rev. Lett. **84**, 4023 (2000).

[49] C. Cohen-Tannoudji and D. Guéry-Odelin, *Advances in Atomic Physics: An Overview* (World Scientific, Singapore, 2011).

[50] M. I. Makin, J. H. Cole, C. D. Hill, and A. D. Greentree, Phys. Rev. Lett. **108**, 017207 (2012).